



Published in final edited form as:

J Cogn Neurosci. 2011 December ; 23(12): 4022–4037. doi:10.1162/jocn_a_00077.

Behavioral Interpretations of Intrinsic Connectivity Networks

Angela R. Laird¹, P. Mickle Fox¹, Simon B. Eickhoff^{2,3}, Jessica A. Turner⁴, Kimberly L. Ray¹, D. Reese McKay¹, David C. Glahn⁵, Christian F. Beckmann⁶, Stephen M. Smith⁶, and Peter T. Fox¹

¹University of Texas Health Science Center, San Antonio

²RWTH Aachen University

³Research Center Jülich

⁴The Mind Research Network, Albuquerque, NM

⁵Institute of Living and Yale University, Hartford, CT

⁶University of Oxford

Abstract

An increasingly large number of neuroimaging studies have investigated functionally connected networks during rest, providing insight into human brain architecture. Assessment of the functional qualities of resting state networks has been limited by the task-independent state, which results in an inability to relate these networks to specific mental functions. However, it was recently demonstrated that similar brain networks can be extracted from resting state data and data extracted from thousands of task-based neuroimaging experiments archived in the BrainMap database. Here, we present a full functional explication of these intrinsic connectivity networks at a standard low order decomposition using a neuroinformatics approach based on the BrainMap behavioral taxonomy as well as a stratified, data-driven ordering of cognitive processes. Our results serve as a resource for functional interpretations of brain networks in resting state studies and future investigations into mental operations and the tasks that drive them.

INTRODUCTION

Intrinsic connectivity networks (ICNs) have emerged as fundamental, organizational elements of human brain architecture. Following the discovery of functionally correlated fMRI time series present during rest (Cordes et al., 2000; Xiong, Parsons, Gao, & Fox, 1999; Biswal, Yetkin, Haughton, & Hyde, 1995), ICNs have been consistently identified in multivariate decompositions of fMRI data using independent component analysis (ICA; Allen et al., 2011; Zuo et al., 2010; van den Heuvel, Mandl, Kahn, & Hulshoff Pol, 2009; Damoiseaux et al., 2006; De Luca, Beckmann, De Stefano, Matthews, & Smith, 2006; Beckmann, DeLuca, Devlin, & Smith, 2005; van de Ven, Formisano, Prvulovic, Roeder, & Linden, 2004; Kiviniemi, 2003). We recently reported that ICA of thousands of activation studies produces coactivation networks that are strikingly similar to resting state networks (Smith et al., 2009). The term “intrinsic connectivity network” (Seeley et al., 2007), therefore, expands upon the concept of resting state networks to include the set of large-scale functionally connected brain networks that can be captured in either resting state or

task-based neuroimaging data. The evidence presented by Smith et al. (2009) affirms that the functional organization of the brain can be differentiated into spatially distinct modes that are not limited to rest but extend to active states. Because of the task-independent nature of the resting state, previous assessment of ICN functions has been imprecise, relying on impressionistic naming gleaned from component similarity to task-based results. In contrast, the BrainMap database (brainmap.org) offers an innovative opportunity for automated functional interpretation of ICNs. In the present study, we examine the full set of BrainMap behavioral descriptors at a standard low order decomposition to create quantifiable descriptions of ICNs and identify which fields carry the most explanatory power in delineating functional differences between networks.

Behavior is the critical variable regulated in all functional neuroimaging experiments. To evoke and isolate a cognitive domain of interest, investigators design paradigms in which the stimulus, response, or instructions are categorically or parametrically modulated. Precise manipulation of all experimental variables ensures the identification of brain regions associated with the underlying behavior. The BrainMap taxonomy (Fox et al., 2005) records these experimental manipulations as textual metadata to link brain activations with their associated mental operations. BrainMap's database structure, thus, allows the quantitative determination of how strongly each ICN relates to a given task or mental process. Here, we demonstrate that ICNs map to different metadata combinations relevant to cognition, emotion, perception, interoception, and action, indicating that these networks are responsible for functionally unique operations. This systematic mining of BrainMap metadata provided a substantially richer characterization of ICNs than has been previously possible.

Metadata exploration was carried out using hierarchical clustering analysis (HCA) to sort both behavioral groupings and networks into similar clusters. Combined application of two data-driven analyses was performed to test our theory that independent brain (ICA) and behavior (HCA) analyses yield limited insight into functional brain architecture but jointly facilitate new knowledge discovery in cognitive neuroscience. We hypothesized that our results would yield some function–structure correlations that align with well-established primary system organization (e.g., motor, visual, auditory) and that other results would provide more complex insight into higher domains of cognition and multi-sensory integration. As predicted by Smith et al. (2009), we set forth a framework for deriving a neuroimaging-driven cognitive ontology and establish that this strategy is extremely powerful when pursued in the context of intrinsic connectivity. Our results serve as a resource for future interpretations of brain networks in resting state studies, which potentially will provide significant contributions to understanding functional connections spanning the entire brain.

METHODS

The BrainMap Database

The BrainMap database (Laird, Lancaster, & Fox, 2005, 2009; Fox & Lancaster, 2002) is an on-line repository of published functional neuroimaging results. Reduced data are archived in BrainMap in the form of three-dimensional coordinates in stereotactic space (x,y,z) extracted from the peak locations of reported brain activations in the literature, similar to other databases such as SumsDB (Van Essen, 2009), AMAT (Hamilton, 2009), and Brede (Nielsen, 2009; Nielsen & Hansen, 2002). For each experiment, the target brain template utilized during the spatial normalization procedure is recorded to allow renormalization to a standard brain space, thereby facilitating the meta-analytic comparison of coordinates across studies. BrainMap currently supports analyses in either Talairach (Talairach & Tournoux, 1988) or Montreal Neurological Institute (MNI; Collins, Neelin, Peters, & Evans, 1994) standard spaces. In the present study, coordinates were analyzed in Talairach space;

conversions between spaces were carried out using the Lancaster transform (Laird et al., 2010; Lancaster et al., 2007).

BrainMap currently archives coordinates from approximately 20% of the functional neuroimaging literature (Derrfuss & Mar, 2009), along with behavioral metadata extracted over 67 coding fields, resulting in a total of nearly 1.4 million instantiations of BrainMap metadata. Our analyses were carried out on peak coordinates and metadata associated with 8637 functional brain imaging experiments, which were extracted from 1840 publications that reported 69,481 activation locations across 31,724 subjects. Subject ages ranged from 1 to 90 years old (mean of reported group mean age = 31.5 years), which included studies reporting brain activations in men only (22%), women only (8%), and mixed gender groups (70%).

Generation of Intrinsic Connectivity Maps

Peak coordinates in BrainMap were smoothed using a Gaussian distribution (FWHM = 12 mm) to accommodate the spatial uncertainty associated with neuroimaging foci and generate modeled activation images with 2-mm resolution (Figure 1, Step 1). This smoothing has been shown to provide a reasonable approximation to the whole brain statistical parametric images from which they were extracted (Eickhoff et al., 2009; Salimi-Khorshidi, Smith, Keltner, Wager, & Nichols, 2009). ICA (dimensionality $d = 20$) was applied to this 4D data (Space \times Experiment ID) using MELODIC (multivariate exploratory linear optimized decomposition into independent components; Beckmann et al., 2005) in FSL (FMRIB Software Library; Woolrich et al., 2009; Smith et al., 2004) to decompose the experiment images into 20 spatially independent components, which represent the major modes of coactivation across the BrainMap database (Figure 1, Step 2). A dimensionality of 20 was chosen to provide continuity of comparison with our previous report involving ICA of BrainMap experiment images (Smith et al., 2009). Along with each spatial map, a corresponding experiment ID vector was generated that describes how strongly a given component relates to each of the original 8637 experiment images. ICA maps were converted to z statistic images via a normalized mixture model fit, thresholded at $z > 4$, and viewed on a Talairach space template image (Kochunov et al., 2002).

The BrainMap Taxonomy

The BrainMap behavioral taxonomy of functional neuroimaging studies includes 67 descriptor fields (f), which are described in Supplementary Table 1. These fields relate information concerning the citation, subjects, conditions, and experiments (defined as contrasts of conditions resulting in a statistical parametric image), the latter three of which are critical for establishing how observed brain activation patterns were elicited. A subset of 14 fields was selected to quantify the functional properties of ICNs observed in BrainMap, based on two criteria: (1) structured keyword format, rather than free text entries, and (2) description of functionally relevant metadata (e.g., titles of journals were deemed not relevant to network descriptions). These keyword fields (e.g., “paradigm”) are designated by a list of n classes (e.g., “saccades”) to maintain a structured taxonomy (Supplementary Table 2). The class lists are continually updated to evolve as the database grows but have been structured to maximize the creation of groupings of similar studies and minimize classes that include only one or two studies.

Metadata Matrices

Analysis of the spatial networks using ICA was followed by analysis of the behavioral metadata, following a procedure initially developed by Smith et al. (2009). Given that each activation location in BrainMap maps to a complex set of metadata fields, we utilized the matrix that quantifies the relationship between components and BrainMap experiments to

assess the functional properties of each ICA network. To do this, we computed the matrix M , which is an $e \times d$ matrix whose e rows (one for each experiment) and d columns (one for each ICA component) describe the weightings of each component for each of the original activation images,

$$M = V_d M_d, \quad (1)$$

where V_d includes the d largest singular values of the “temporal” (experiment ID) modes and M_d is the mixing matrix of size $d \times d$. We then extract the n (Metadata class) \times e (Experiment) matrix P from BrainMap and form the final matrix of metadata classes versus ICA maps,

$$P_d = PM. \quad (2)$$

A set of 14 metadata matrices (of size $n \times d$) was computed that corresponded to the 14 independent metadata fields in Supplementary Table 2. These categories included but were not limited to behavioral domain (the cognitive process isolated by the experimental contrast; for example, “working memory”; $n = 50$), paradigm (the type of task or challenge presented to the subject; for example, “ n -back”; $n = 75$), stimulus modality (e.g., “visual,” “auditory”; $n = 7$), stimulus type (e.g., “letters,” “tones”; $n = 38$), response modality (e.g., “hand,” “foot”; $n = 8$), response type (e.g., “button press,” “speech”; $n = 13$), or task instructions (e.g., “generate,” “attend”; $n = 17$). Metadata matrices were normalized by rows to aid visualization and account for uneven sampling across classes in the BrainMap database (e.g., there are more studies in BrainMap that focus on cognition than interoception).

Once the relationships between networks and BrainMap metadata were assessed across all fields, we assessed the relative salience of each field. The maximum value within each component was computed for every metadata class and averaged across classes for each field as a method of identifying if a given metadata field captured a large amount of functional information. The average value, rather than the maximum value, was computed across fields because the high field-wise maximum values can be driven by very high values within a single class, whereas the average value provides a better measure for the range of classes across a given field. Using this approach for computing the salience of all 14 metadata fields, we selected two variables that captured the highest degree of explanatory power, behavioral domain and paradigm, and pursued further unpacking of the ICNs using these fields (Figure 1, Step 3).

Hierarchical Clustering Analysis

To assess groupings of similar metadata classes within behavioral domain and paradigm fields, HCA was performed separately on the two matrices using $1 - r$ as the distance between clusters, where r is the Pearson’s correlation coefficient. The Pearson’s coefficient was chosen over the Spearman rank correlation coefficient so as to preserve column structure of the Metadata \times Component matrices (i.e., metadata pertaining to a given ICN was analyzed in comparison with metadata from a different ICN). Similar dendrograms were obtained when analyzing the 50 behavioral domains and 75 paradigm classes separately; therefore, these fields were concatenated and HCA was performed on the combined metadata matrix of 125 metadata classes \times 20 networks. Clustering was first performed on the combined matrix to determine groupings across domains and paradigms; we subsequently transposed the matrix and repeated the analysis to quantify similarity across ICNs (Figure 1, Step 4). Clustering for both dimensions was performed in MATLAB (Natick, MA) using three different methods that differ in how they measure the distance

between clusters. The “single” method utilizes the shortest distance, “complete” utilizes the furthest distance, and “average” utilizes the unweighted averaged distance. The same results were consistently obtained across these three clustering methods, indicating high reliability of our results; here, we present the results obtained using the “single” method.

RESULTS

Functional interpretation of ICNs proceeded in two stages, first by identifying networks via spatial analysis of Brain-Map peak coordinates and then by characterizing their functions via analysis of BrainMap behavioral metadata. Figure 2 displays the ICA results of images modeled within BrainMap using previously developed methods (Smith et al., 2009), in which sets of peak foci were decomposed into 20 spatially co-occurring ICN maps (for additional slices, see Supplementary Figure 1). We expected to observe small differences in spatial topographies compared with the ICA decomposition of BrainMap data performed by Smith et al. (2009) because of the expanded data set available in the present study (i.e., 7342 activation images were included in 2009, whereas 8637 images were analyzed here). This prediction was confirmed when we observed that 17 components in Smith et al. (2009) exactly matched 17 components in the present data set. Of the remaining three components, two were split or merged from existing components, and one was novel to the previous analysis. Despite this minor variation in results, *all* of the components identified in the present data set have been observed in other ICA-based studies of resting state and intrinsic connectivity (Allen et al., 2011; Zuo et al., 2010; Robinson et al., 2009; Smith et al., 2009; van den Heuvel et al., 2009; Calhoun, Kiehl, & Pearlson, 2008; Damoiseaux et al., 2006; De Luca et al., 2006; Beckmann et al., 2005).

A recent study by Biswal et al. (2010) describes the decomposition of a very large resting fMRI data set (306 subjects) using ICA at the same standard low dimensionality that was chosen here ($d = 20$). When comparing the resting state networks observed by Biswal et al. (2010) to the BrainMap coactivation networks described here, we found that 12 of the nonartifactual components were an excellent match whereas four components were a close partial match. An example of a partially matching network is the default mode network, which was observed as a single component in our analysis (ICN 13), but split into posterior (IC 6) and anterior (IC 13) components in Biswal et al. (2010), a decomposition that has been frequently observed in default mode studies (Laird, Eickhoff, et al., 2009; Uddin, Kelly, Biswal, Xavier Castellanos, & Milham, 2009; Damoiseaux et al., 2006). Therefore, only 2 of 20 components in the present data (ICNs 5 and 9) showed no correspondence with the networks presented by Biswal et al. (2010), demonstrating stronger agreement between resting state and activation networks than observed by Smith et al. (2009). This higher degree of correspondence can likely be attributed to the much larger sample size of the resting state analysis (i.e., 36 subjects analyzed by Smith et al., 2009 vs. 306 subjects by Biswal et al., 2010).

In the previous study by Smith et al. (2009), the discussion of functional network properties was limited to the 10 well-matched pairs of networks that were observed. Of the remaining 10 networks, two were found to be artifactual (identical to the analysis presented here) and eight were judged to be “of more complex interpretation” and omitted from further discussion. However, as these networks have all been observed in previous decompositions of resting state fMRI data, we sought to determine the full functional explication of the entire set of observed components at a low order decomposition, as described below.

Metadata Matrices

To quantitatively assess the functional specializations of the observed ICN, we examined the per-experiment contributions to each component across 14 different BrainMap metadata

fields. Metadata matrices describing the weightings of each component for each metadata class were generated for these functionally relevant fields and are visualized as heat maps (Supplementary Figures 2–13). In these images, positive matrix values indicate metadata classes that are correlated with a given BrainMap network, and negative values indicate classes that are decorrelated, in the sense that these metadata classes were not observed across the corresponding experiments. We are cautious in not drawing overly significant interpretations of the negative values because they result from mathematical artifacts associated with explicit and implicit data demeaning in ICA and are not derived from negative values in the original data. However, they do offer potentially interesting information on the relationships between functionally exclusive metadata classes. The matrices depicted a unique composite of mental operations, revealing that the 20 ICNs differed not only anatomically, but also functionally.

Hierarchical Clustering Analysis

We determined that the behavioral domain and paradigm contained the most explanatory power of the 14 metadata fields by computing the maximum matrix value within each metadata class and averaging across all classes for a given field, because a high value indicates a large amount of functional information was captured (Figure 3). HCA of the concatenated behavioral domain and paradigm matrix was first performed to determine clustering across domains and paradigms; we subsequently transposed the matrix and repeated the analysis to quantify similarity across ICNs. Figure 4 details the first set of HCA results as a dendrogram that reflects the linear dependence of any two metadata classes (a high-resolution version is available at brainmap.org/icns/dendrogram). Larger bins along the x axis (e.g., “Action,” “Language”) indicate clusters of multiple behavioral domains and paradigms with congruous themes. For example, a strong link was observed between numerous affective and interoceptive processes, suggesting that these processes are driven by similar neural substrates. Individually labeled rows (e.g., “Deception Task”) indicate incompatible classes that did not fall within a well-defined cluster. The far right of Figure 4 thus includes a number of tasks with unique functional bases that were not found to cluster within any other group. For example, neuroeconomics as elicited by “Delay Discounting” tasks was found to be strongly dissimilar to any other metadata.

The second set of HCA results provided data-driven groupings across ICA components and revealed three clusters of networks displaying high similarity, along with a divergent set of dissimilar networks (Figure 5). The corresponding behavioral domain and paradigm metadata for the three similar network clusters revealed dominant functional themes of emotion and interoception, motor and visuospatial processing and coordination, and vision. The set of dissimilar networks was composed of five networks with well-defined cognitive functions on an individual basis but lacking in a collective theme. The composite metadata matrix for behavioral domains and paradigms was then reordered to reflect the classifications set forth by these clustering results to provide optimal visualization and interpretation of the functional properties associated with each ICN. The corresponding set of relationships is displayed as a heat map in Figure 6 (a high-resolution version is available at brainmap.org/icns/heatmap).

Functional Interpretation of Networks

We provide the following functional explication of each ICN. To fully describe the structural extent of each network, we employ multiple nomenclatures, including anatomical (e.g., “precentral gyrus,” “thalamus”), directional (e.g., “dorsolateral pFC”), functional (e.g., “primary motor cortex”; “M1”), and cytoarchitectonic (e.g., “Brodmann’s area 32”). The use of these different labeling schemas is intended as communicative technique to report the anatomical regions encompassed by each spatial map. In particular, use of the Brodmann’s

area terminology is not meant to describe specific cytoarchitectonic boundaries but is used as a macroscopic indicator of inexact boundaries to provide the reader with an estimation of the anatomical locations of the ICNs.

Group 1: ICNs 1–5—The networks grouped in cluster 1 of Figure 5 were strongly related to a collective range of emotional and autonomic processes. These processes included interoceptive challenges related to thirst, viewing of sexually explicit or highly emotional pictures or films, and recall of emotional autobiographical memories. This category also included gustation and olfaction, which are technically classified under “Perception” under the BrainMap taxonomy, but it is likely that these classes were strongly clustered to interoception given their strong link to the autonomic responses of hunger and thirst, rather than to truly exteroceptive processes of mechanoreception or proprioception.

- ICN 1 (limbic and medial-temporal areas) included primary olfactory and limbic association cortices (BA 28/34/ 35/36/38), including parahippocampal gyri. This network was strongly associated with discrimination of emotional faces and pictures, particularly those that elicited fear, happiness, or humor. In addition, ICN 1 was strongly weighted toward interoceptive processing elicited during air-hunger and, more weakly, olfactory and gustatory responses.
- ICN 2 (subgenual ACC and OFC) included BA 25 and BA 10/ 11/12 and was loaded toward olfaction, gustation, and emotion, with a strong preference for reward and thirst tasks.
- ICN 3 (bilateral BG and thalamus) was found to be linked to a wide range of mental processes, most strongly to reward tasks, nonpainful thermal stimulation, and interoceptive functions (e.g., bladder, sexuality, hunger, and thirst). In addition, this network was also found to be relevant to motor, pain, and somatosensory processing, with preference for a few cognitive tasks such as classical conditioning, go/no-go, film viewing, syntactic discrimination, and delay discounting. ICN 3 was additionally associated with emotional tasks, most strongly to anxiety as well as with olfaction and TMS.
- ICN 4 (bilateral anterior insula/frontal opercula and the anterior aspect of the body of the cingulate gyrus) encompassed BA 13/16 and BA 24. These regions accounted for a complex set of language, executive function, affective, and interoceptive processes corresponding to the Stroop, go/ no-go, Flanker, and Simon tasks, as well as auditory, pain, and gustatory processes. Other paradigms included deception, music, and classical conditioning. This wide range of network functions was elicited across all possible stimulus modalities. Given the heterogeneous range of functions associated with ICN 4, we consider it to be a transitional network linking cognition and emotion/interoception.
- ICN 5 (midbrain) demonstrated strong, restricted loadings to acupuncture and air-hunger tasks. This network was also weakly linked to sensorimotor functions and autonomic processes relevant to the bladder. Experiments reporting activations within this network were strongly weighted toward interoceptive stimulation.

Group 2: ICNs 6–9—The second cluster of networks was driven by a mixture of functions related to motor and visuospatial integration, coordination, and execution.

- ICN 6 (superior and middle frontal gyri) included the premotor and supplementary motor cortices (SMA; BA 6) and FEFs (BA 8/9) and was related to cognitive control of visuomotor timing and preparation of executed movements. Strongly weighted behavioral domains included action imagination and preparation and

visual motion, and important paradigms were the Flanker task, saccades, antisaccades, and the learning and recall of complex sequences. Stimulus types tended toward visual targets, fixation points, and LEDs, to which subjects were frequently instructed to fixate, imagine, and track.

- ICN 7 (middle frontal gyri and superior parietal lobules) included dorsolateral prefrontal (BA 46) and posterior parietal cortices (BA 7) involving visuospatial processing and reasoning, with a strong weighting for tasks such as the Wisconsin Card Sorting Test, saccades, antisaccades, mental rotation, and counting or calculation. Notably, metadata functions for ICNs 7 and 4 agree with the systems differentiated in a dual-network model of top-down attentional control proposed by Dosenbach et al. (2007) wherein fronto-parietal and cinguloopercular networks are responsible for adaptive control and stable maintenance functions, respectively.
- ICN 8 (ventral precentral gyri, central sulci, postcentral gyri, superior and inferior cerebellum) included primary sensorimotor cortices for upper extremities (M1; S1; BA 4/3/1/2). This network was associated with action and somesthesia corresponding to hand movements and included tasks such as finger tapping, grasping, pointing, electrical and vibrotactile stimulation, and TMS.
- ICN 9 (superior parietal lobule) included the medial posterior parietal association area (BA 5). This network was not observed as a separate component in our previous analysis (Smith et al., 2009) but split from the previous ICN 8 component (hand region of the primary sensorimotor cortex) because of the increased number of papers in BrainMap accumulated between analyses. Support for the decomposition of ICNs 8 and 9 into two separate components is provided by a previous study indicating that medial superior parietal cortex (BA 5) is functionally distinct from primary sensorimotor cortices (Scheperjans, Grefkes, Palomero-Gallagher, Schleicher, & Zilles, 2005). Interestingly, the heat map for this network was strongly negative, indicating the range of cognitive and emotional functions that were anticorrelated, rather than correlated, with this region. A weak positive preference was found for motor execution and learning, particularly involving drawing and reaching, in agreement with previous research on the integration of body movements and hand-eye coordination (Andersen & Cui, 2009; Creem-Regehr, 2009).

Group 3: ICNs 10–12—This cluster encompassed three networks related to visual perception.

- ICN 10 (middle and inferior temporal gyri) included the middle temporal visual association area (MT, MST, V5; BA 37/39) at the temporo-occipital junction. This network was elicited by viewing complex, often emotional, stimuli (e.g., faces, films), as well as action observation, overt picture naming, and visual tracking of moving objects, particularly random dot formations. Other tasks included mental rotation and the discrimination of locations in space.
- ICNs 11 and 12 (lateral and medial posterior occipital cortices) included the primary, secondary, and tertiary visual cortices (V1, V2, V3; BA 17/18/19). When viewed together, ICNs 12, 11, and 10 extended from medial to lateral aspects of the occipital and temporal cortices. ICN 12 was strongly linked to simple visual stimuli such as flashing checkerboards, and ICN 11 involved higher-level visual processing associated with orthography and covert reading. ICN 11 also corresponded to Braille reading, demonstrating observed plasticity of these cortical regions in blind subjects. ICNs 11 and 12 displayed relatively weak loadings across many fields, such as behavioral domain, paradigm, and several of the condition fields (Figure 3).

Rather than reflect a functional nonspecialization, further inspection of the heat map for the field “experimental contrast” revealed that many reported activations in these lateral and medial visual networks resulted from experiments in which the visual stimulation was not properly controlled. Because these visual activation patterns were not the primary effect sought and were classified under some other functional class (e.g., a delayed match to sample task contrasted with a resting baseline would be classified with a behavioral domain of “working memory,” not “vision”), the functional descriptors relating to vision were, therefore, diluted across other metadata classes.

Divergent Networks: ICNs 13–18—Following the clustering of ICN groups 1–3, which displayed high within-group component similarity, we observed several divergent networks that demonstrated strong dissimilarity to the three previous groups and to each other. The exception to this trend was found for ICNs 16 and 17, which were coupled together, although not to the degree seen across groups 1–3.

- ICN 13 (medial prefrontal and posterior cingulate/precuneus areas) was the component known as the default mode network and strongly corresponded to theory of mind and social cognition tasks. Weaker correspondence was observed for fixation, episodic recall, imagined scenes, and delay discounting tasks.
- ICN 14 (cerebellum), commonly associated with action and somesthesia, demonstrated a distributed range of sensorimotor, autonomic, and cognitive functions. Interestingly, both overt and covert naming showed a preference for cerebellar activity, despite the fact that no other language or speech tasks were associated with this region. Similarly ICN 14 showed preference for processing of humorous stimuli, yet no other emotional responses were observed.
- ICN 15 (right-lateralized fronto-parietal regions) included right BA 44/45 and 22/39/40. This network involved multiple cognitive processes, such as reasoning, attention, inhibition, and memory, and showed preference for *n*-back, delay discounting, and divided auditory attention tasks.
- ICN 16 (transverse temporal gyri) included the primary auditory cortices (A1; BA 41/42) and was related to audition (including tone and pitch discrimination), music, and speech. Other processes included phonological discrimination and oddball discrimination.
- ICN 17 (dorsal precentral gyri, central sulci, postcentral gyri, superior and inferior cerebellum) included primary sensorimotor cortices for mouth (M1, S1; BA 4/3/1/2) and was associated with action and somesthesia corresponding to speech, such as overt reading or recitation, chewing or swallowing, and flexion/extension of the tongue.
- ICN 18 (left-lateralized fronto-parietal regions) included Broca’s (BA 44/45) and Wernicke’s (BA 22/39/40) areas and strongly mapped to a host of semantic, phonologic, and orthographic language tasks such as word generation and covert reading, as well as working and explicit memory tasks, such as paired associate recall, cued encoding and recognition, and the Sternberg task. Surprisingly, this network displayed a stronger preference toward working memory than did ICN 7. Stimulus types included words, pseudowords, letters, and Asian characters, with a dominance of button press responses.

Artifacts: Components 19–20—Artifactual resting state networks following ICA decompositions have been previously attributed to respiratory and cardiac functions (Zuo et

al., 2010; Smith et al., 2009). Although these specific artifacts are not pertinent when analyzing co-occurring activation networks using peak coordinates, we did observe artifacts of a different origin.

- Components 19 and 20 were characterized by uniformly distributed metadata maps that showed no preference for any domain of brain function. Instead, ICN 19 corresponds to template mismatch errors in BrainMap that occur when recording standard brain space of reported locations (i.e., MNI or Talairach coordinates). MNI brains are approximately 20% larger than individual subject brains (Lancaster et al., 2007), and inaccurate classification of standard space results in substantial errors during coordinate-based meta-analyses, with the largest errors lying in superior frontal and inferior cortices (Laird et al., 2010; Lancaster et al., 2007). Given that ICN 19 includes voxels that rim the outer boundaries of the brain, particularly in the inferior direction, it is reasonable to assume that ICN 19 results from MNI foci erroneously flagged as Talairach coordinates, typically because of ambiguous reporting standards in the literature. ICN 20, although not as immediately identifiable as artifact as ICN 19, similarly includes voxels near the edge of the brain, particularly in the right superior frontal cortex. The origin of this component is difficult to characterize, but an abnormally high number of experiments in this component utilized MedX software to normalize their data to Talairach space, indicating that ICN 20 is potentially because of some algorithmic abnormality occurring during spatial normalization.

Validation of Metadata Clustering

Given the observed complex clustering of behavioral domains and paradigms in Figure 4, we investigated if a similar dendrogram could be obtained outside the context of networks driven by intrinsic connectivity. To this end, we extracted the metadata matrix of behavioral domains and paradigms directly from the experiments in the BrainMap database (8637 experiments \times 125 metadata classes), which was free of any effects related to the functional organization of ICNs. Clustering this matrix yielded a uniform and highly dissimilar dendrogram characterized by very little branching and minimal organizational structure (Figure 7). Important structural differences between the dendrograms in Figures 3 and 7 are apparent in the large discrepancy in *y*-axis scaling (maximum dissimilarity metric of 0.45 and 0.90, respectively). When measuring how well a dendrogram reflects a given data set, it is useful to compare the original distance data to the cophenetic distances, where for any two classes the cophenetic distance is the distance between the two clusters that contain those two classes, represented by the link height in the cluster tree. High correlation between original distances and cophenetic distances indicates valid clustering models. We computed the cophenetic correlation coefficient for the dendrogram derived from clustering based on brain–behavior correlations (Figure 4; $\alpha_{bb} = 0.5119$) and compared it to that associated with behavior alone (Figure 7; $\alpha_b = 0.3516$). A cophenetic correlation coefficient of 1 indicates a perfect clustering solution; therefore, the dendrogram associated with ICNs reflected a more accurate approximation to the given data set. Closer inspection of the dendrogram driven by behavior alone reflected the trivial co-occurrences of tasks and processes associated with experimental design trends. For example, one cluster indicated that when a task utilizes a paradigm of “Music Comprehension/Production,” it is typically coded in BrainMap with a behavioral domain of “Cognition.Music”. These simple paradigm–domain pairs were observed throughout the behavior-alone dendrogram and overall did not convey the rich complexity of relationships between tasks and processes that was observed for the brain–behavior dendrogram. Thus, we conclude a significant functional advantage to joint analysis of brain and behavior information, as opposed to analysis of behavior alone.

DISCUSSION

We examined the epistemological potential of ICNs via large-scale mining of the BrainMap database, motivated by recent evidence relating these networks to functional brain architecture (Smith et al., 2009). ICA was applied at a standard low model order to determine spatial groupings of brain regions, whereas HCA identified behavioral groupings of cognitive tasks and processes. Spatial topographies of the BrainMap networks more closely matched the set of resting state networks observed in a recent large-scale analysis of 306 subjects (Biswal et al., 2010) than observed by Smith et al. (2009), and it is likely that the higher degree of correspondence is a result of the increased sample size. The innovation behind the present study lies in the joint analyses of brain networks and behavioral metadata, which yielded both anatomical localization of networks as well as the automated characterization of their functional properties in a manner not possible in resting state data. Minimal organizational structure was discerned when behavior was analyzed independently, as demonstrated in HCA before extraction of ICNs wherein we observed superficial and limited pairings of a few domains and paradigms that merely reflect the way tasks are constructed (e.g., *n*-back tasks elicit working memory). To this extent, consideration of behavior alone captures only a summary of experimental design trends, rather than the complex and meaningful set of relationships illustrated in Figure 4.

Low-level Unimodal Processing

We successfully predicted that unimodal processing domains relevant to audition, action, and vision would be clearly isolated to well known neural systems, providing a strong metric of success for our method. Primary auditory cortices localized to ICN 16, with strong behavioral relationships to audition and music. Similarly, primary motor cortices mapped to basic sensorimotor tasks, but localized to two different ICNs corresponding to somatotopic mapping of the hand (ICN 8) or mouth (ICN 17). More complex visuomotor coordination was separately extracted to ICN 6 in the supplementary motor and premotor cortices and FEFs. This simple-to-complex motor organization was mirrored in the visual system in ICNs 12 (medial visual cortices), 11 (lateral visual cortices), and 10 (middle temporal visual area), in which correlated stimuli progressed from flashing checkerboards to complex visual shapes and letters to emotional or moving presentations of faces or pictures. Rather than a strict spatial decomposition for primary, secondary, or tertiary visual cortices, we instead observed a medial to lateral delineation of networks that has been replicated in numerous resting state analyses (Allen et al., 2011; Zuo et al., 2010; Smith et al., 2009; Calhoun et al., 2008; Damoiseaux et al., 2006; De Luca et al., 2006; Beckmann et al., 2005), with functional properties that agree with previous evidence for retinotopic organization differentiating macular and full field stimulus presentations (e.g., words vs. checkerboard patterns; Fox et al., 1986).

High-level Cognitive Processing

Predictions that high-level cognitive processes would involve neural systems demonstrating more complex and less evident behavioral segregations were also confirmed. Our results included some known neural relationships of cognition, such as ICN 18, which was left lateralized to Broca's and Wernicke's areas and displayed a strong preference for language and memory tasks. Other results were less unequivocal and indicate a potential in these analyses for generating new hypotheses in cognitive neuroscience. For example, we were curious to see if commonly held theories concerning the organizational roles of brain areas relevant to executive function could be substantiated by the present results. Specifically, we were interested if the right inferior frontal gyrus was related to inhibition, anterior cingulate to response conflict, and lateral prefrontal and parietal cortices to working memory. Our results do confirm these trends (ICNs 15, 4, and 7, respectively), but with additional

specifications. Two ICNs were linked to inhibition, possibly because of separate components for cognitive (ICN 15) and motor (ICN 6) processing. Cognitive control related to stimulus and response conflict as induced by the Stroop, Simon, and Flanker tasks was strongly related to ICN 4, as expected, but ICNs 18 and 6 were also associated with these tasks, perhaps as a result of task differences associated with verbal and visuospatial processing. Multiple classes of working memory tasks mapped to lateral prefrontal and parietal cortices (ICN 7), yet ICN 18 demonstrated a relatively stronger mapping to these processes that may reflect a more significant reliance on articulatory rehearsal (Badre & Wagner, 2007; Chein, Fissell, Jacobs, & Fiez, 2002; Smith & Jonides, 1999). Relative dissociation was observed for the loadings for the *n*-back, delayed match to sample, and Sternberg tasks across ICNs 7, 15, and 18. The *n*-back task was strongly loaded for all three of these networks, but restricted mainly to ICN 18 for delayed match to sample and Sternberg tasks, indicating important network differences between continuous updating and recalling of stimulus information. Lastly, we noted an overall ontological segregation between specific processes related to executive functioning, with relative dissimilarity between clusters associated with working memory and reasoning and those of inhibition and attention (Figure 4). These classifications suggest that localization differences associated with separate executive function subdomains may be quite profound.

Interesting results relevant to higher-level cognition were also observed in the cerebellum. Cerebellar function has been intensely debated for a century, with numerous divergent theories related to motor coordination and timing, motor learning, sensory integration, or higher cognitive processing. Our results indicated highly distributed functions of the cerebellum, with limited specialization. One explanation is that the cerebellum is implicated in such a diverse range of polymodal processes that it may be responsible for a spectrum of processes rather than a unique function or perhaps functions as a coprocessing node (Bower, 1997).

Clustering of Networks

The network groupings observed in Figure 5 are potentially one of the more valuable findings of this study. Often, the results of a neuroimaging network decomposition are reported by organizing subsets of networks into functionally similar groups. This is generally done in a purely qualitative manner, relying on authors' knowledge of basic neural systems. Typically, a group is easily identified for visual networks and another for motor networks. Beyond this, the groupings greatly vary and often include both functional (e.g., "default mode," "attention," or "executive function" networks) and anatomical (e.g., "BG," "frontal-parietal," "cerebellar" networks) nomenclatures. However, the unique nature of BrainMap metadata allows us to demonstrate a new approach, in which the groupings were driven solely by metadata correlations that reveal similar task patterns across networks, with no bias reflecting our particular knowledgebase of functional systems. Here, we provide a quantitative evaluation of how network functions can be grouped, with an informative assessment of the way in which some groups are strongly correlated in function (e.g., vision and motor) and other groups are not (e.g., the divergent cognitive networks).

Model Order and Other Approaches

The purpose of the current study was to address the lack of functional labels for ICNs. Although previous work has addressed component selection and quantitative discrimination between networks and artifactual components (Sui, Adali, Pearlson, & Calhoun, 2009; De Martino et al., 2007), the present study provides innovative quantitative labeling of component functions. The present analysis focused solely on ICA at a standard low dimensionality of 20 components to allow for straightforward comparisons to the networks observed in other resting state ICA studies in the literature, the majority of which utilize a

low model order. We were particularly interested in facilitating comparisons to the 20 networks identified by Biswal et al. (2010) and Smith et al. (2009), given the high significance of their findings. Our previous work (Smith et al., 2009) included the initial description of the functional labeling method presented here but provided minimal descriptions of the network functions. We have addressed this potential ambiguity in behavioral interpretations by expanding to include all observed networks using the full extent of BrainMap metadata. These results thus allow for a clearer explication of the functional associations that can be inferred regarding the ICA networks derived from a standard low order decomposition. By fully developing a method for behavioral interpretations of ICNs at a low model order, we aim to link this work to current resting state studies and provide a bridge to future BrainMap ICA studies that integrate an expanded view of the human connectome across multiple dimensionalities. Therefore, further investigations concerning the spatial and functional network patterns at much higher dimensions are currently being explored ($d = 100, 150, \text{ and } 200$) using these methods, which relate to previous work in repeated decompositions of resting state data (Abou-Elseoud et al., 2010; Kiviniemi et al., 2009). As suggested by Smith et al. (2009), these high model order analyses have the potential to provide valuable insight into the organizational hierarchy for networks and subnetworks across the full range of the human connectome. However, these more fine-grained analyses result in a large and complex set of networks that can potentially be difficult and cumbersome to interpret. Our efforts here to clarify the functional differences between observed low-dimensionality networks will likely be critical for comparative analyses of results at higher dimensions.

Meta-analytic connectivity modeling (MACM) is a method that offers results that are similar to the coactivation-based results seen in high model order ICA decompositions; however, it is based on regionally specific questions, as opposed to the whole-brain network approach presented here. In MACM, the coactivation patterns associated with a ROI are queried across the BrainMap database and analyzed to determine if any functional parcellation can be identified based on differential patterns of whole-brain connectivity across a range of tasks. This method has been used to assess functional connectivity of the amygdala (Robinson, Laird, Glahn, Lovallo, & Fox, 2010) and parietal operculum (Eickhoff et al., 2010), as well as regions of the default mode network (Laird, Eickhoff, et al., 2009). These analyses have focused on a single region or network, which has allowed a deep examination of the connectivity and metadata-based assessment of function. In future studies, we aim to determine to what extent the results of fine-grained MACM studies match the results of ICA decompositions at high model order. Similarly, we aim to investigate the comparative results that can be obtained via non-meta-analytic, seed-based resting state functional connectivity analyses. Previously, this method has been utilized to investigate the parcellation of networks associated with a number of brain regions, such as the anterior cingulate (Margulies et al., 2007), medial-temporal cortex (Roy et al., 2009; Kahn, Andrews-Hanna, Vincent, Snyder, & Buckner, 2008), posteromedial cortex (Cauda et al., 2010; Margulies et al., 2009), medial frontal cortex (Kim et al., 2010), cerebellum (O'Reilly, Beckmann, Tomassini, Ramnani, & Johansen-Berg, 2010; Krienen & Buckner, 2009), and insula (Deen, Pitskel, & Pelphrey, in press; Cauda et al., 2011). The data and analyses in the present study offer an alternative technique for simultaneously investigating multiple sets of functional brain networks, as well as a more quantitative method for querying the functional significance associated with those sets of networks.

Implications for Neuroinformatics

These results suggest that the current neuroinformatics methodology offers a wealth of opportunities for generating novel brain-behavior hypotheses and stimulating future research studies. In addition, the coupled analyses of spatial and behavioral metadata from

the BrainMap database generated an ordering strategy for human behaviors and the tasks that drive them and provided a potential framework for future development of a cognitive ontology (Poldrack, 2006; Price & Friston, 2005). Neuroimaging ontology development, particularly relevant to human cognition and behavior, is relatively underdeveloped in comparison with other large-scale biomedical fields that rely heavily on informatics, such as genomics (Jones, Pizarro, Spellman, Miller, & FuGE Working Group, 2006; Whetzel et al., 2006). This represents a critical gap for the neuroimaging community because the development of computer-based knowledge representations capable of automated reasoning across concepts in cognitive neuroscience will likely encourage future large-scale data-driven meta-analyses similar to, but more powerful than, what has been accomplished here.

The current analysis provides evidence that the overall design and scope of the BrainMap taxonomy can support development of a brain-behavior ontology. However, we observed limitations in which BrainMap terms did not fully capture the functional properties of a network, suggesting that future metadata expansion is warranted. For example, Figure 6 illustrates the lack of strong metadata peaks across ICN 14 in the cerebellum and ICN 5 in the midbrain. This imprecision was most notable for ICN 9, which revealed an extremely small number of positive metadata correlations accompanied by a large extent of negative correlations. As previously noted, these ambiguous results may not be because of term granularity but rather classification techniques across experimental contrasts, as demonstrated in the reduced functional specialization of the networks associated with visual processing (ICNs 11 and 12). A few BrainMap terms did not strongly map to any specific network (e.g., color discrimination), whereas some classes mapped equally well to multiple networks. This was exemplified in sequence recall and motor learning, which strongly mapped to both ICN 6 (SMA) and ICN 8 (hand region of primary motor cortex) and potentially implicates the multinet network involvement across different components of action execution. Future work will also involve expanding the BrainMap taxonomy to ascertain if functionally significant network differences can be discriminated at greater levels of resolution. Data-driven refinement of classes and related terms may be accomplished by applying text-mining analyses directly to publications reporting the experimental results that contribute to each network. Such a strategy would retain the strengths of the present analysis by driving ontology development in the context of ICNs but improve the current framework by introducing author-defined terms originating from domain-specific knowledge.

Similarly, the extent of functional insight to be realized from BrainMap's metadata correlations is potentially limited by the ontological complications of developing a formal representation for functional neuroimaging results. For example, a word generation experiment may utilize a silent reading baseline, whereas another, a resting baseline, yet both of these experiments will be coded in BrainMap under the same paradigm class regardless of the different activation patterns that are to be expected from these different contrasts. In the current analysis, we did not attempt to disentangle this ambiguity, which potentially limits our results. It is feasible that, using our above example, the word generation results were potentially split across multiple components, which would mean that the functional significance of different control conditions was not identified. However, given that each contrast is coded as utilizing either a low-level or high-level baseline condition, future analyses may be pursued to examine the effect of including this parameter when interpreting ICA results. It is highly possible that dissociable network patterns may be observed that reflect the different processes that are isolated for low-level versus high-level contrasts.

Data Sharing

The network images and associated metadata generated in this study have been made available for download (brainmap.org/icns) to serve as a shared community resource for

interpreting the functional significance of future resting state results. In addition, they may be useful as masks for seeding specific a priori cortical regions or networks of interest in prospective neuroimaging studies or as a technique for circumventing the inherent problems associated with double dipping (Kriegeskorte, Simmons, Bellgowan, & Baker, 2009). Coordinate-based results that were analyzed to generate maps of intrinsic connectivity are available in the BrainMap database and can be accessed using the Sleuth application (brainmap.org/sleuth).

Supplementary Material

Refer to Web version on PubMed Central for supplementary material.

Acknowledgments

This work was supported by NIMH grants R01-MH074457 (P. T. F. and A. R. L.) and R01-MH084812 (A. R. L. and J. A. T.) and the Helmholtz Initiative on Systems-Biology (S. B. E.).

REFERENCES

- Abou-Elseoud A, Starck T, Remes J, Nikkinen J, Tervonen O, Kiviniemi V. The effect of model order selection in group PICA. *Human Brain Mapping*. 2010; 31:1207–1216. [PubMed: 20063361]
- Allen EA, Erhardt EB, Damaraju E, Gruner W, Segall JM, Silva RF, et al. A baseline for the multivariate comparison of resting state networks. *Frontiers in Neuroscience*. 2011; 5:2. [PubMed: 21441979]
- Andersen RA, Cui H. Intention, action planning, and decision making in parietal-frontal circuits. *Neuron*. 2009; 63:568–583. [PubMed: 19755101]
- Badre D, Wagner AD. Left ventrolateral prefrontal cortex and the cognitive control of memory. *Neuropsychologia*. 2007; 45:2883–2901. [PubMed: 17675110]
- Beckmann CF, DeLuca M, Devlin JT, Smith SM. Investigations into resting-state connectivity using independent component analysis. *Philosophical Transactions of the Royal Society of London, Series B, Biological Sciences*. 2005; 360:1001–1013.
- Biswal B, Yetkin FZ, Haughton VM, Hyde JS. Functional connectivity in the motor cortex of resting human brain using echo-planar MRI. *Magnetic Resonance in Medicine*. 1995; 34:537–541. [PubMed: 8524021]
- Biswal BB, Mennes M, Zuo XN, Gohel S, Kelly C, Smith SM, et al. Toward discovery science of human brain function. *Proceedings of the National Academy of Sciences, U.S.A.* 2010; 107:4734–4739.
- Bower JM. Is the cerebellum sensory for motor's sake, or motor for sensory's sake? *Progress in Brain Research*. 1997; 114:463–496. [PubMed: 9193161]
- Calhoun VD, Kiehl KA, Pearlson GD. Modulation of temporally coherent brain networks estimated using ICA at rest and during cognitive tasks. *Human Brain Mapping*. 2008; 29:828–838. [PubMed: 18438867]
- Cauda F, D'Agata F, Sacco K, Duca S, Geminiani G, Vercelli A. Functional connectivity of the insula in the resting brain. *Neuroimage*. 2011; 55:8–23. [PubMed: 21111053]
- Cauda F, Geminiani G, D'Agata F, Sacco K, Duca S, Bagshaw AP, et al. Functional connectivity of the posteromedial cortex. *PLoS One*. 2010; 5:e13107. [PubMed: 20927345]
- Chein JM, Fissell K, Jacobs S, Fiez JA. Functional heterogeneity within Broca's area during verbal working memory. *Physiology & Behavior*. 2002; 77:635–639. [PubMed: 12527011]
- Collins DL, Neelin P, Peters TM, Evans AC. Automatic 3D intersubject registration of MR volumetric data in standardized Talairach space. *Journal of Computer Assisted Tomography*. 1994; 18:192–205. [PubMed: 8126267]
- Cordes D, Haughton VM, Arfanakis K, Wendt GJ, Turski PA, Moritz CH, et al. Mapping functionally related regions of brain with functional connectivity MR imaging. *American Journal of Neuroradiology*. 2000; 21:1636–1644. [PubMed: 11039342]

- Creem-Regehr SH. Sensory-motor and cognitive functions of the human posterior parietal cortex involved in manual actions. *Neurobiology of Learning and Memory*. 2009; 91:166–171. [PubMed: 18996216]
- Damoiseaux JS, Rombouts SA, Barkhof F, Scheltens P, Stam CJ, Smith SM, et al. Consistent resting-state networks across healthy subjects. *Proceedings of the National Academy of Sciences, U.S.A.* 2006; 103:13848–13853.
- De Luca M, Beckmann CF, De Stefano N, Matthews PM, Smith SM. fMRI resting state networks define distinct modes of long-distance interactions in the human brain. *Neuroimage*. 2006; 29:1359–1367. [PubMed: 16260155]
- De Martino F, Gentile F, Esposito F, Balsi M, Di Salle F, Goebel R, et al. Classification of fMRI independent components using IC-fingerprints and support vector machine classifiers. *Neuroimage*. 2007; 34:177–194. [PubMed: 17070708]
- Deen B, Pitskel NB, Pelphrey KA. Three systems of insular functional connectivity identified with cluster analysis. *Cerebral Cortex*. (in press).
- Derrfuss J, Mar RA. Lost in localization: The need for a universal coordinate database. *Neuroimage*. 2009; 48:1–7. [PubMed: 19457374]
- Dosenbach NU, Fair DA, Miezin FM, Cohen AL, Wenger KK, Dosenbach RA, et al. Distinct brain networks for adaptive and stable task control in humans. *Proceedings of the National Academy of Sciences, U.S.A.* 2007; 104:11073–11078.
- Eickhoff S, Jbabdi S, Caspers S, Laird AR, Fox PT, Zilles K, et al. Anatomical and functional connectivity of cytoarchitectonic areas within the human parietal operculum. *Journal of Neuroscience*. 2010; 30:6409–6421. [PubMed: 20445067]
- Eickhoff SB, Laird AR, Grefkes C, Wang LE, Zilles K, Fox PT. Coordinate-based activation likelihood estimation meta-analysis of neuroimaging data: A random-effects approach based on empirical estimates of spatial uncertainty. *Human Brain Mapping*. 2009; 30:2907–2926. [PubMed: 19172646]
- Fox PT, Laird AR, Fox SP, Fox PM, Uecker AM, Crank M, et al. BrainMap taxonomy of experimental design: Description and evaluation. *Human Brain Mapping*. 2005; 25:185–198. [PubMed: 15846810]
- Fox PT, Lancaster JL. Mapping context and content: The BrainMap model. *Nature Reviews Neuroscience*. 2002; 3:319–321.
- Fox PT, Mintun MA, Raichle ME, Miezin FM, Allman JM, Van Essen DC. Mapping human visual cortex with positron emission tomography. *Nature*. 1986; 323:806–809. [PubMed: 3534580]
- Hamilton AF. Lost in localization: A minimal middle way. *Neuroimage*. 2009; 48:8–10. [PubMed: 19442743]
- Jones AR, Pizarro A, Spellman P, Miller M. FuGE Working Group. FuGE: Functional genomics experiment object model. *OMICS*. 2006; 10:179–184. [PubMed: 16901224]
- Kahn I, Andrews-Hanna JR, Vincent JL, Snyder AZ, Buckner RL. Distinct cortical anatomy linked to subregions of the medial temporal lobe revealed by intrinsic functional connectivity. *Journal of Neurophysiology*. 2008; 100:129–139. [PubMed: 18385483]
- Kim JH, Lee JM, Jo HJ, Kim SH, Lee JH, Kim ST, et al. Defining functional SMA and pre-SMA subregions in human MFC using resting state fMRI: Functional connectivity-based parcellation method. *Neuroimage*. 2010; 49:2375–2386. [PubMed: 19837176]
- Kiviniemi V. Independent component analysis of nondeterministic fMRI signal sources. *Neuroimage*. 2003; 19:253–260. [PubMed: 12814576]
- Kiviniemi V, Starck T, Remes J, Long X, Nikkinen J, Haapea M, et al. Functional segmentation of the brain cortex using high model order group PICA. *Human Brain Mapping*. 2009; 30:3865–3886. [PubMed: 19507160]
- Kochunov P, Lancaster J, Thompson P, Toga AW, Brewer P, Hardies J, et al. An optimized individual target brain in the Talairach coordinate system. *Neuroimage*. 2002; 17:922–927. [PubMed: 12377166]
- Kriegeskorte N, Simmons WK, Bellgowan PS, Baker CI. Circular analysis in systems neuroscience: The dangers of double dipping. *Nature Neuroscience*. 2009; 12:535–540.

- Krienen FM, Buckner RL. Segregated frontocerebellar circuits revealed by intrinsic functional connectivity. *Cerebral Cortex*. 2009; 19:2485–2497. [PubMed: 19592571]
- Laird AR, Eickhoff SB, Li K, Robin DA, Glahn DC, Fox PT. Investigating the functional heterogeneity of the default mode network using coordinate-based meta-analytic modeling. *Journal of Neuroscience*. 2009; 29:14496–14505. [PubMed: 19923283]
- Laird AR, Lancaster JL, Fox PT. BrainMap: The social evolution of a human brain mapping database. *Neuroinformatics*. 2005; 3:65–78. [PubMed: 15897617]
- Laird AR, Lancaster JL, Fox PT. Lost in localization? The focus is meta-analysis. *Neuroimage*. 2009; 48:18–20. [PubMed: 19559800]
- Laird AR, Robinson JL, McMillan KM, Tordesillas-Gutiérrez D, Moran ST, Gonzales SM, et al. Comparison of the disparity between Talairach and MNI coordinates in functional neuroimaging data: Validation of the Lancaster transform. *Neuroimage*. 2010; 51:677–683. [PubMed: 20197097]
- Lancaster JL, Tordesillas-Gutiérrez D, Martinez M, Salinas F, Evans A, Zilles K, et al. Bias between MNI and Talairach coordinates analyzed using the ICBM-152 brain template. *Human Brain Mapping*. 2007; 28:1194–1205. [PubMed: 17266101]
- Margulies DS, Kelly AM, Uddin LQ, Biswal BB, Castellanos FX, Milham MP. Mapping the functional connectivity of anterior cingulate cortex. *Neuroimage*. 2007; 37:579–588. [PubMed: 17604651]
- Margulies DS, Vincent JL, Kelly C, Lohmann G, Uddin LQ, Biswal BB, et al. Precuneus shares intrinsic functional architecture in humans and monkeys. *Proceedings of the National Academy of Sciences, U.S.A.* 2009; 106:20069–20074.
- Nielsen FA. Lost in localization: A solution with neuroinformatics 2.0? *Neuroimage*. 2009; 48:11–13. [PubMed: 19497377]
- Nielsen FA, Hansen LK. Modeling of activation data in the BrainMap database: Detection of outliers. *Human Brain Mapping*. 2002; 15:146–156. [PubMed: 11835605]
- O'Reilly JX, Beckmann CF, Tomassini V, Ramnani N, Johansen-Berg H. Distinct and overlapping functional zones in the cerebellum defined by resting state functional connectivity. *Cerebral Cortex*. 2010; 20:953–965. [PubMed: 19684249]
- Poldrack RA. Can cognitive processes be inferred from neuroimaging data? *Trends in Cognitive Sciences*. 2006; 10:59–63. [PubMed: 16406760]
- Price CJ, Friston KJ. Functional ontologies for cognition: The systematic definition of structure and function. *Cognitive Neuropsychology*. 2005; 22:262–275. [PubMed: 21038249]
- Robinson JL, Laird AR, Glahn DC, Lovallo WR, Fox PT. Meta-analytic connectivity modeling: Delineating the functional connectivity of the human amygdala. *Human Brain Mapping*. 2010; 31:173–184. [PubMed: 19603407]
- Robinson S, Basso G, Soldati N, Sailer U, Jovicich J, Bruzzone L, et al. A resting state network in the motor control circuit of the basal ganglia. *BMC Neuroscience*. 2009; 10:137. [PubMed: 19930640]
- Roy AK, Shehzad Z, Margulies DS, Kelly AMC, Uddin LQ, Gotimer K, et al. Functional connectivity of the human amygdala using resting state fMRI. *Neuroimage*. 2009; 45:614–626. [PubMed: 19110061]
- Salimi-Khorshidi G, Smith SM, Keltner JR, Wager TD, Nichols TE. Meta-analysis of neuroimaging data: A comparison of image-based and coordinate-based pooling of studies. *Neuroimage*. 2009; 45:810–823. [PubMed: 19166944]
- Scheperjans F, Grefkes C, Palomero-Gallagher N, Schleicher A, Zilles K. Subdivisions of human parietal area 5 revealed by quantitative receptor autoradiography: A parietal region between motor, somatosensory, and cingulate cortical areas. *Neuroimage*. 2005; 25:975–992. [PubMed: 15808998]
- Seeley WW, Menon V, Schatzberg AF, Keller J, Glover GH, Kenna H, et al. Dissociable intrinsic connectivity networks for salience processing and executive control. *Journal of Neuroscience*. 2007; 27:2349–2356. [PubMed: 17329432]
- Smith EE, Jonides J. Storage and executive processes in the frontal lobes. *Science*. 1999; 283:1657–1661. [PubMed: 10073923]

- Smith SM, Fox PT, Miller KL, Glahn DC, Fox PM, Mackay CE, et al. Correspondence of the brain's functional architecture during activation and rest. *Proceedings of the National Academy of Sciences, U.S.A.* 2009; 106:13040–13045.
- Smith SM, Jenkinson M, Woolrich MW, Beckmann CF, Behrens TE, Johansen-Berg H, et al. Advances in functional and structural MR image analysis and implementation as FSL. *Neuroimage*. 2004; 23(Suppl. 1):S208–S219. [PubMed: 15501092]
- Sui J, Adali T, Pearlson GD, Calhoun VD. An ICA-based method for the identification of optimal fMRI features and components using combined group-discriminative techniques. *Neuroimage*. 2009; 46:73–86. [PubMed: 19457398]
- Talairach, J.; Tournoux, P. Co-planar stereotaxic atlas of the human brain: 3-Dimensional proportional system: An approach to cerebral imaging. Stuttgart: Georg Thieme; 1988.
- Uddin LQ, Kelly AM, Biswal BB, Xavier Castellanos F, Milham MP. Functional connectivity of default mode network components: Correlation, anticorrelation, and causality. *Human Brain Mapping*. 2009; 30:625–637. [PubMed: 18219617]
- van, de; Ven, VG.; Formisano, E.; Prvulovic, D.; Roeder, CH.; Linden, DE. Functional connectivity as revealed by spatial independent component analysis of fMRI measurements during rest. *Human Brain Mapping*. 2004; 22:165–178. [PubMed: 15195284]
- van, den; Heuvel, MP.; Mandl, RC.; Kahn, RS.; Hulshoff Pol, HE. Functionally linked resting-state networks reflect the underlying structural connectivity architecture of the human brain. *Human Brain Mapping*. 2009; 30:3127–3141. [PubMed: 19235882]
- Van Essen DC. Lost in localization-But found with foci?! *Neuroimage*. 2009; 48:14–17. [PubMed: 19481158]
- Whetzel PL, Brinkman RR, Causton HC, Fan L, Field D, Fostel J, et al. Development of FuGO: An ontology for functional genomic investigations. *OMICS*. 2006; 10:199–204. [PubMed: 16901226]
- Woolrich MW, Jbabdi S, Patenaude B, Chappell M, Makni S, Behrens T, et al. Bayesian analysis of neuroimaging data in FSL. *Neuroimage*. 2009; 45:S173–S186. [PubMed: 19059349]
- Xiong J, Parsons LM, Gao JH, Fox PT. Interregional connectivity to primary motor cortex revealed using MRI resting state images. *Human Brain Mapping*. 1999; 8:151–156. [PubMed: 10524607]
- Zuo XN, Kelly C, Adelman JS, Klein DF, Castellanos FX, Milham MP. Reliable intrinsic connectivity networks: Test-retest evaluation using ICA and dual regression approach. *Neuroimage*. 2010; 49:2163–2177. [PubMed: 19896537]

References

This article has been cited by:

1. Meda, Shashwath A.; Gill, Adrienne; Stevens, Michael C.; Lorenzoni, Raymond P.; Glahn, David C.; Calhoun, Vince D.; Sweeney, John A.; Tamminga, Carol A.; Keshavan, Matcheri S.; Thaker, Gunvant; Pearlson, Godfrey D. Differences in Resting-State Functional Magnetic Resonance Imaging Functional Network Connectivity Between Schizophrenia and Psychotic Bipolar Probands and Their Unaffected First-Degree Relatives. *Biological Psychiatry*. 2012
2. Fox, Peter T.; Friston, Karl J. Distributed processing; Distributed functions? *NeuroImage*. 2012
3. Robinson, Jennifer L.; Laird, Angela R.; Glahn, David C.; Blangero, John; Sanghera, Manjit K.; Pessoa, Luiz; Fox, PMickle; Uecker, Angela; Friehs, Gerhard; Young, Keith A.; Griffin, Jennifer L.; Lovallo, William R.; Fox, Peter T. The functional connectivity of the human caudate: An application of meta-analytic connectivity modeling with behavioral filtering. *NeuroImage*. 2011
4. Conner, Christopher R.; Ellmore, Timothy M.; DiSano, Michael A.; Pieters, Thomas A.; Potter, Andrew W.; Tandon, Nitin. Anatomic and electro-physiologic connectivity of the language system: A combined DTI-CCEP study. *Computers in Biology and Medicine*. 2011

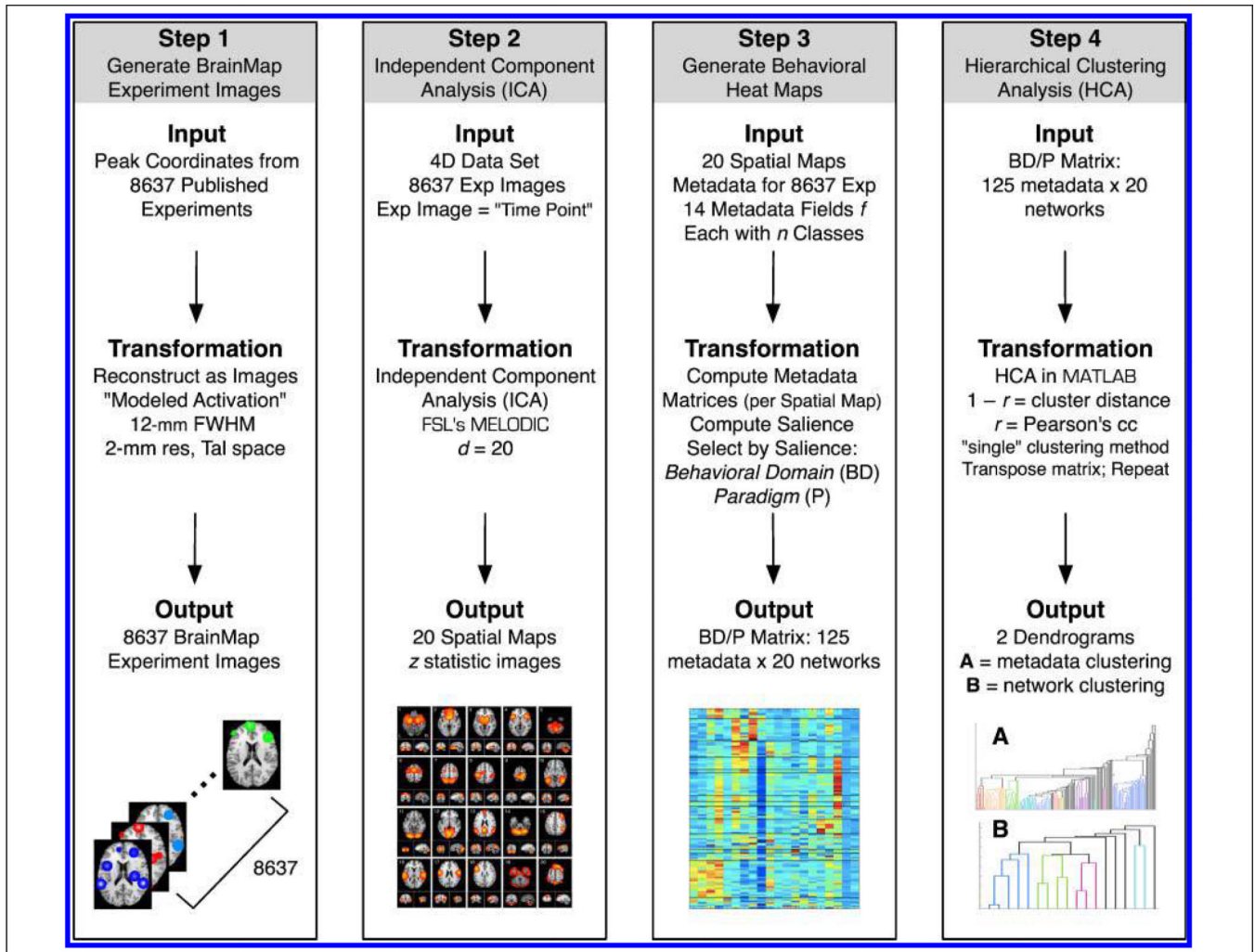


Figure 1.

The data processing pipeline included four steps. Step 1: Peak coordinates in BrainMap were smoothed (12 mm FWHM) to generate 8637 modeled activation images. Step 2: ICA was applied to this 4D data using FSL's MELODIC to decompose the experiment images into 20 spatially independent components. Step 3: The matrix that quantifies the relationship between components and BrainMap experiments was utilized to compute a set of matrices that corresponded to 14 independent metadata fields, each with n classes. The relative saliency as computed for each field and the two fields with the highest saliency were selected for further analysis: behavioral domain and paradigm. Step 4: HCA was performed on the concatenated behavioral domain and paradigm matrix (125 metadata classes \times 20 networks). Clustering was first performed on the combined matrix to determine groupings across metadata classes; subsequently, the matrix was transposed and the analysis repeated to quantify similarity across networks.

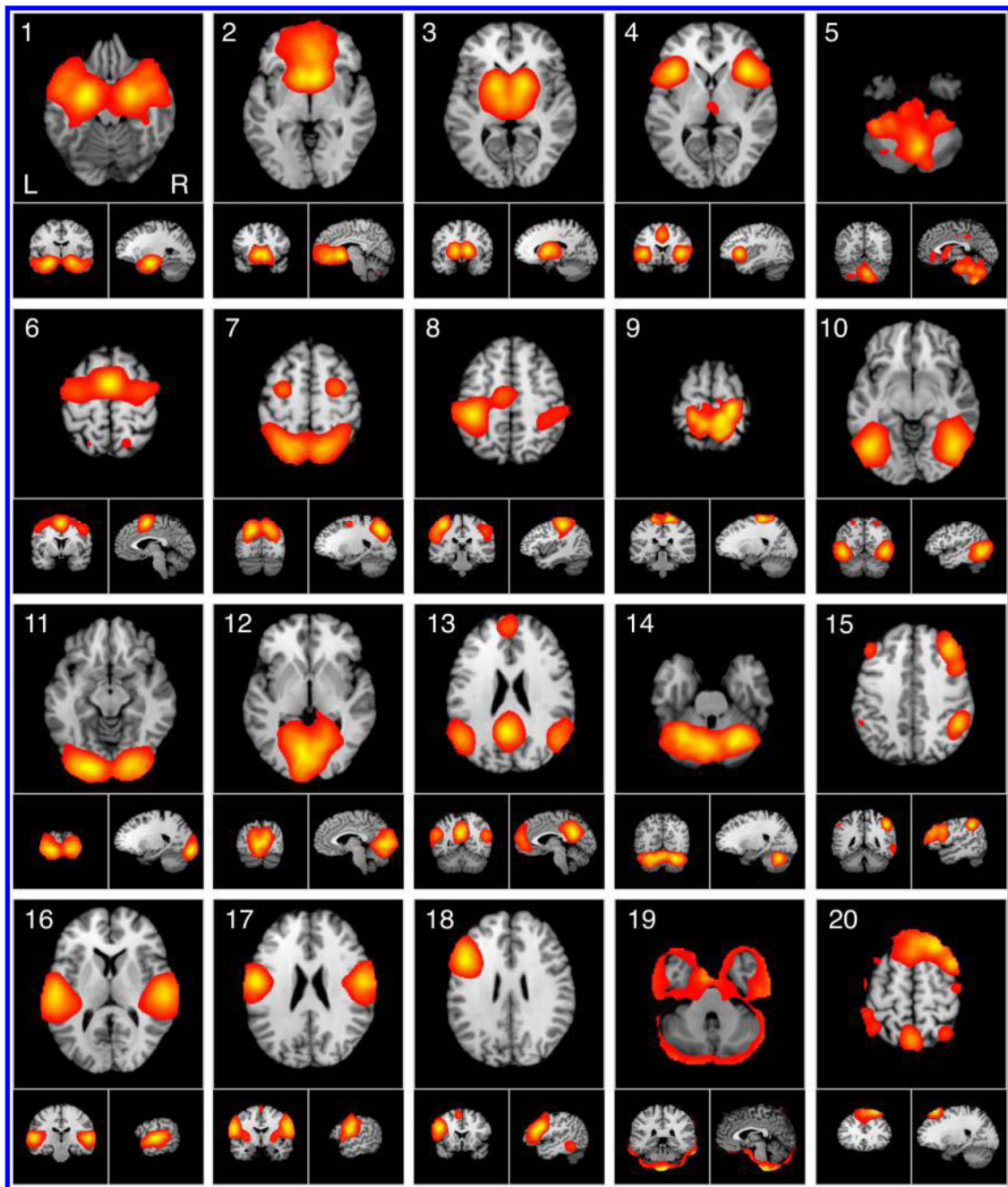


Figure 2.

ICA was used to decompose 8637 experiment images extracted from the BrainMap database into 20 spatially co-occurring maps of ICNs. ICA maps were converted to z statistic images via a normalized mixture model fit, thresholded at $z > 4$, and viewed in standard (Talairach) brain space. Orthogonal slices of the most representative point in space are shown.

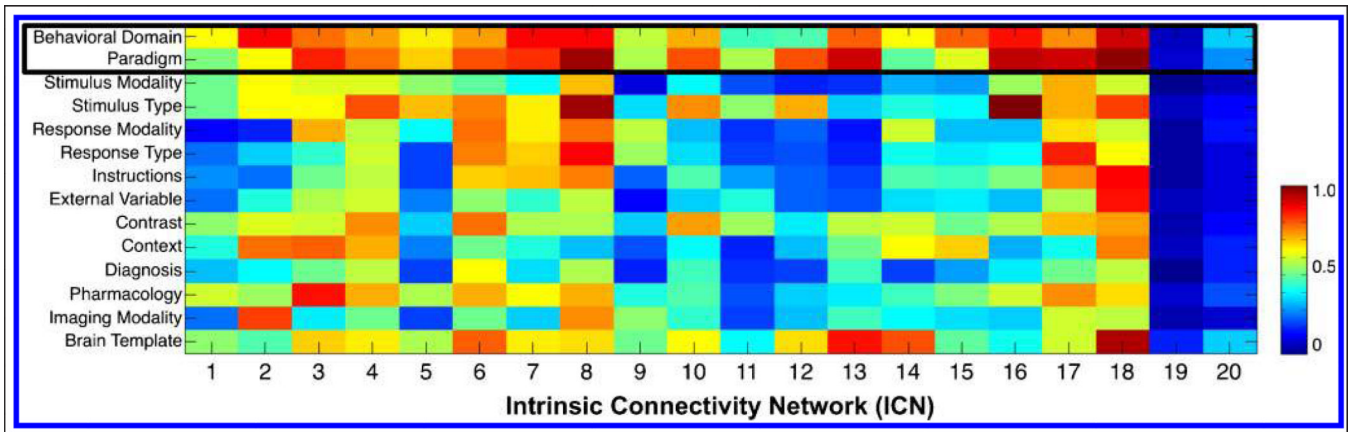


Figure 3.

The maximum metadata loading value across components was computed for every metadata class and averaged across all classes within a given field, as an approach to determine which fields captured a large amount of functional information. We hence identified the behavioral domain and paradigm as the two fields that provided the highest degree of network explanatory power.

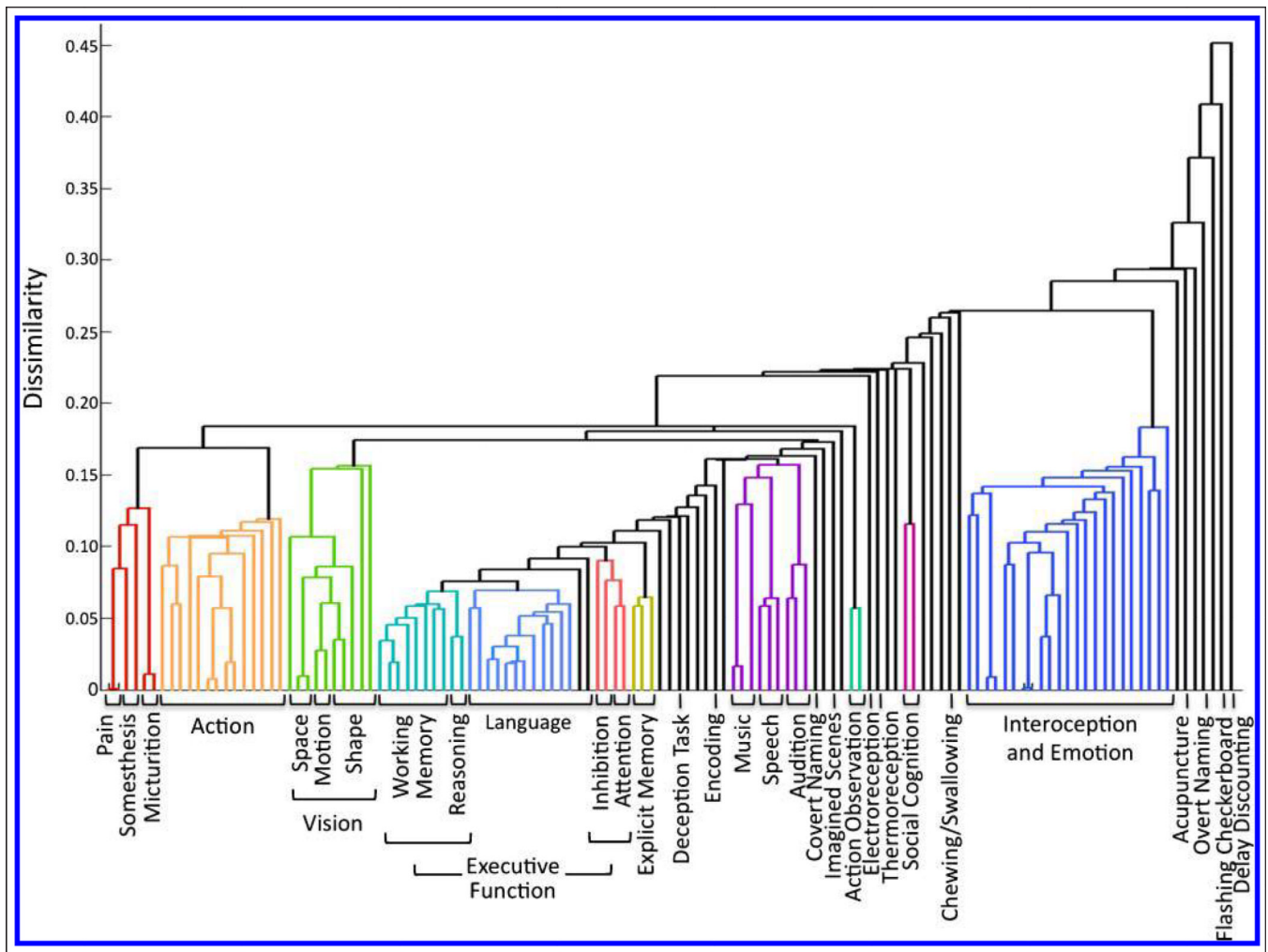


Figure 4. Behavioral-driven HCA was carried out on the metadata matrix of concatenated behavioral domains and paradigms to generate clusters of metadata classes with congruous themes. HCA yielded a complex, well-organized dendrogram associating specific cognitive operations with corresponding experimental paradigms.

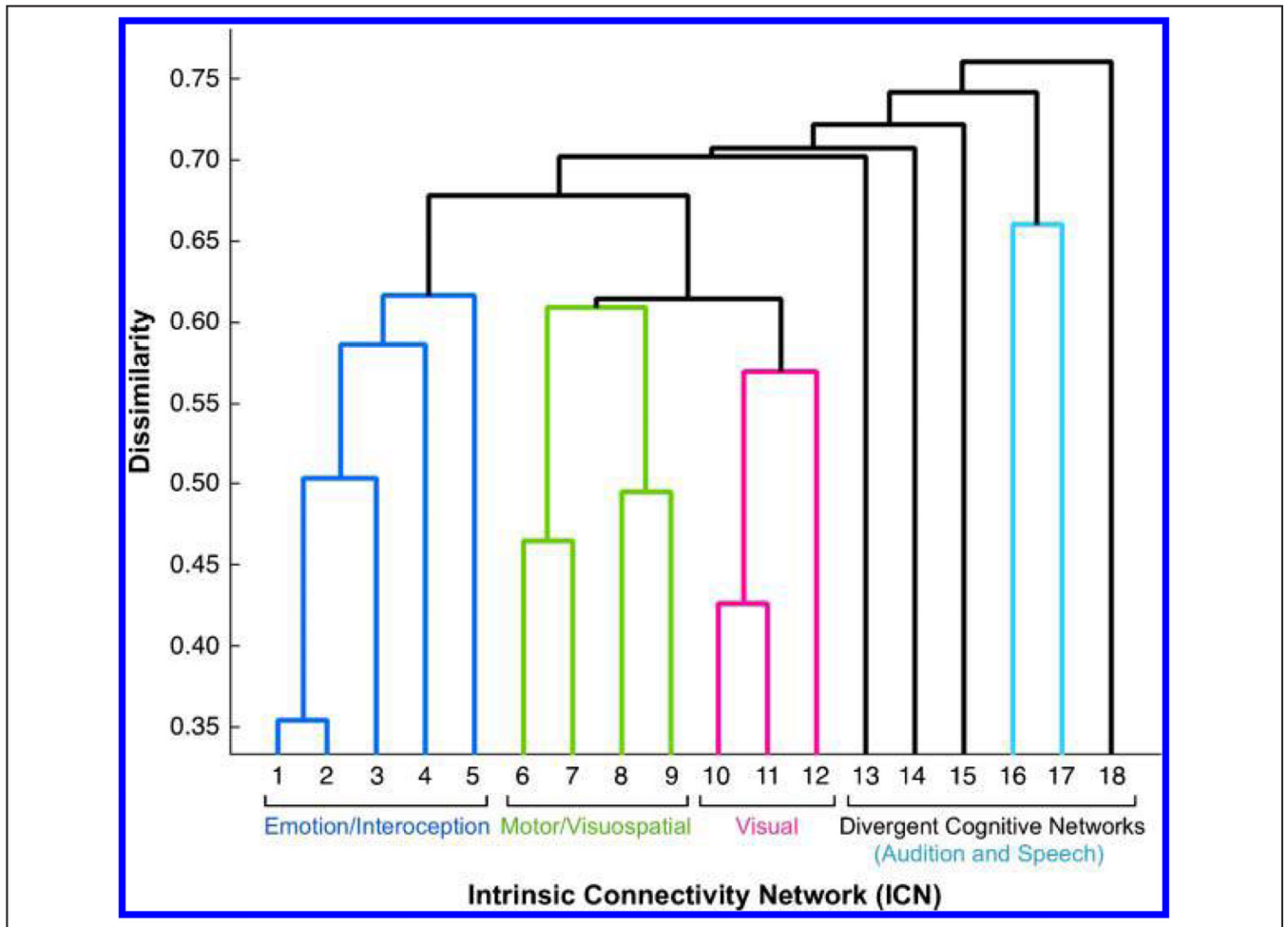


Figure 5.

Network-driven HCA was carried out on the intrinsic connectivity metadata matrix of concatenated behavioral domains and paradigms to generate clusters of networks with function behavioral characterizations. HCA yielded three clusters of networks displaying high similarity (blue, green, red), along with a divergent set of dissimilar networks (black), which included a weakly coupled network pairing (light blue).

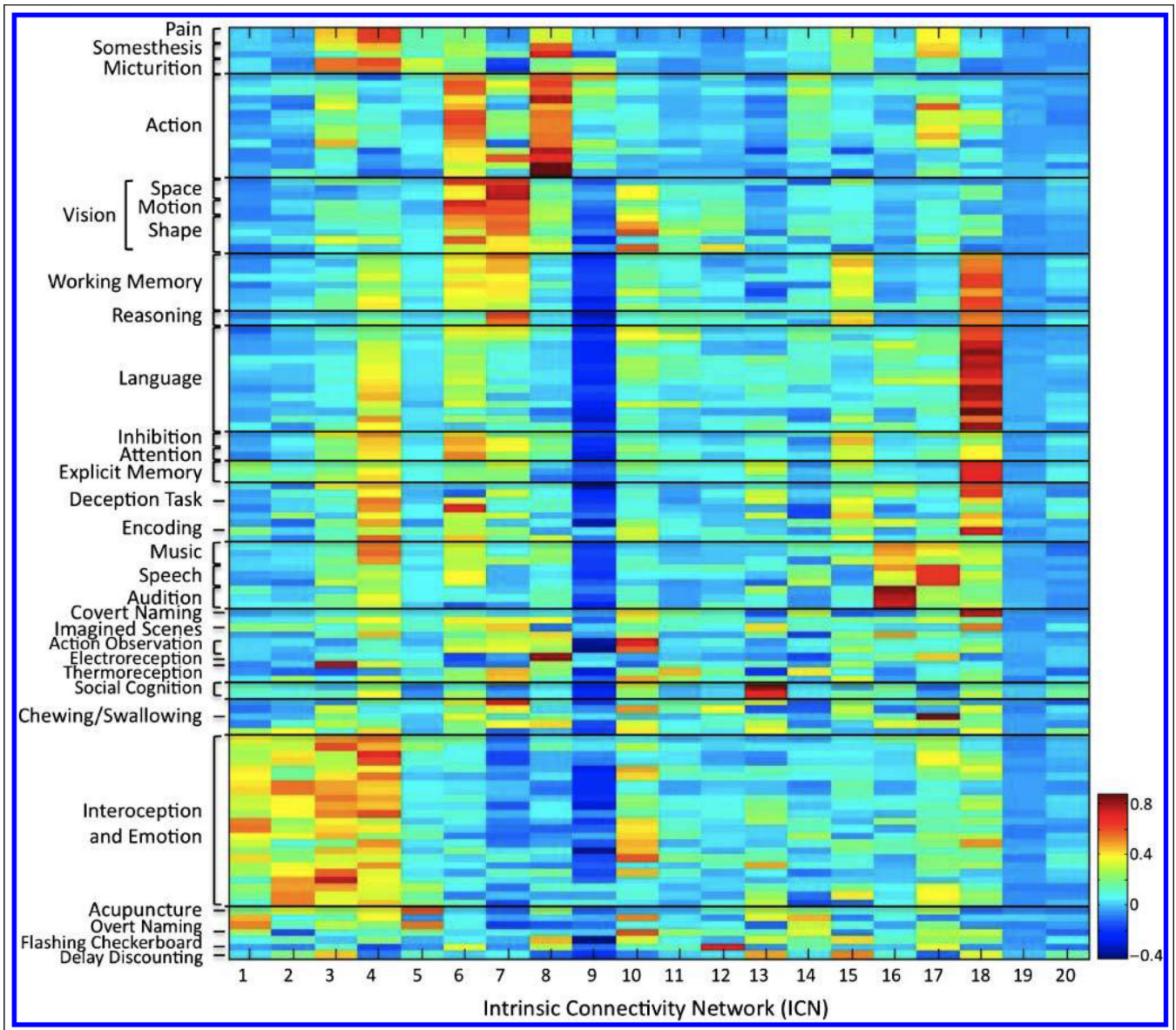


Figure 6.

The concatenated metadata matrix for BrainMap behavioral domains and paradigms provides a per-network mapping of the functional properties of each ICN, ordered to reflect the groupings set forth by the behavioral- and network-driven HCA results.

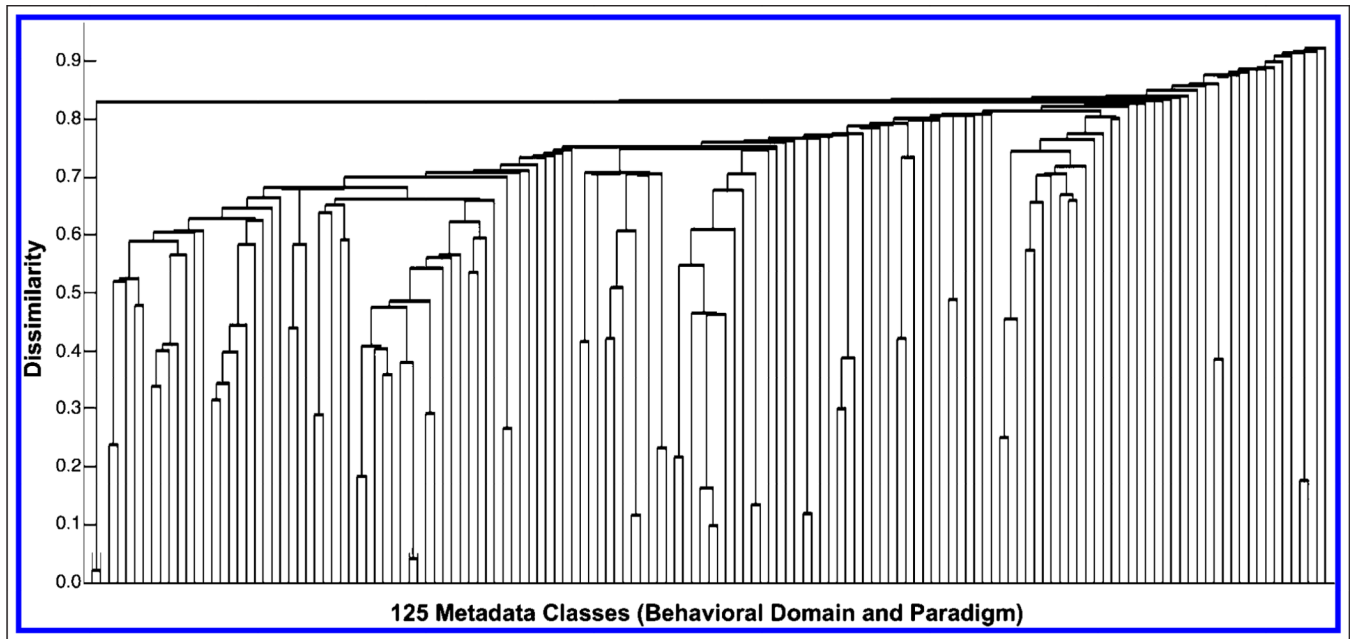


Figure 7.

The metadata matrix of behavioral domains and paradigms was extracted directly from experiments archived in BrainMap (8637 experiments \times 125 metadata classes), without performing ICA on these data. HCA yielded a uniform and highly dissimilar characterized by very little branching and minimal organizational structure. Inspection of this dendrogram revealed a composition based upon simple paradigm–domain pairs that merely reflect trends in experimental design (e.g., *n*-back tasks elicit working memory).